Proceedings 10th NUMGE 2023
10th European Conference on Numerical Methods in Geotechnical Engineering
Zdravkovic L, Kontoe S, Taborda DMG, Tsiampousi A (eds)

https://doi.org/10.53243/NUMGE2023-18

Numerical study of moist tamping and end platens lubrication effect on undrained triaxial test of a sand

M.G. Sottile[1,2], N.A. Labanda[3], R.J. Cier[3], D. Reid[4], A. Fourie[4]

[1]*SRK Consulting, Argentina*
[2]*Universidad de Buenos Aires, Argentina*
[3]*SRK Consulting, Australia*
[4]*University of Western Australia, Australia*

ABSTRACT: Triaxial compression tests are a standard in geotechnical practice due to their usefulness in understanding the mechanical behaviour of the geomaterials and are often used to calibrate constitutive models. When samples are reconstituted in the laboratory, the moist tamping method is usually used to control the global density while enabling the preparation of loose states; however, results from X-ray tomography reported in the literature suggest that the internal density profile entails inhomogeneities. Another important aspect is the lubrication of the end platens; rough ends can lead to dead zones and strain localization within the sample. These two aspects are rarely considered when calibrating constitutive model parameters, as Gauss point elemental tests are generally performed to fit the lab test results. This paper presents a numerical investigation of the moist tamping technique and lubrication end platen effects on the undrained triaxial compression behaviour of the Hutchenson Sand. Sixteen cases are modelled using NorSand constitutive model for different lubrication conditions, sample preparation methods, and pre-shearing average state parameters. Results show that they play a key role in the post-peak behaviour of the material and that Gauss point simulations can only be matched when the sample is perfectly uniform with lubricated ends.

Keywords: Moist tamping, Triaxial test, Numerical modelling, State parameter, Critical state, NorSand

1 INTRODUCTION

Triaxial compression tests are a standard in geotechnical practice due to their usefulness in understanding the mechanical behaviour of the materials and in defining their governing properties (e.g. strength, stiffness, critical state line). Moreover, they are often used to calibrate constitutive models for numerical modelling.

When samples are reconstituted in the laboratory, the moist tamping technique is usually used to control global density while enabling the preparation of loose states. However, results reported in the literature suggest that the internal density profile can entail significant inhomogeneities driven by the layered sample preparation. Thompson and Wong (2008) performed a pioneer work by tracking the initial void ratio distribution and its evolution during undrained shearing of Ottawa Sand (C778) using X-ray computed tomography. The authors reconstituted samples using the moist tamping and water pluviation methods and measured their response for isotropically consolidated undrained triaxial compression and extension tests (CIUC and CIUE, respectively).

Another important aspect of triaxial testing is end restraint. Many authors have advocated the use of end lubrication (Rowe and Barden 1964, Bishop and Green 1965, Lee 1978. Industry comparison programs indicate that lubrication is commonly employed in the study of tailings (e.g. Reid et al. 2021). Further, it has been emphasised that the lubricated ends must be of larger diameter than the specimen to allow lateral expansion at the same ends (Vaid et al. 1999), something which is not always carried out in engineering practice even when lubricated ends are used. However, despite such frequent advocation, there is little data on the effect of lubrication on the strengths inferred from loose brittle soils, and what data is available is often contradictory (Lee 1978, Sheng et al. 1997, Sachan 2011, Elena et al. 2019).

These two aspects are rarely considered when calibrating constitutive model parameters, as Gauss point elemental tests are generally performed to fit the lab test results. This calibration approach ignores the known internal meso-mechanical features that will affect the sample global behaviour, thus obtaining parameters that do not reflect the intrinsic material behaviour.

Based on Thompson and Wang (2008) work, Mozaffari et al. (2022) studied the influence of non-uniformities and end-restrain conditions on the drained triaxial compression response of the Hutchinson Sand through 3D numerical models with a series of previously de-

fined non-uniform void ratio patterns. This paper extends their work to evaluate the effect of void ratio non-uniformities from moist tamping and lubrication of end platen effects on the undrained triaxial compression behaviour of the material. Sixteen cases are modelled to account for two different lubrication conditions (full or nil), sample preparation method (moist tamping and perfectly uniform), and pre-shearing average state parameters (- 0.05, 0.00, 0.05 and 0.10). Models consider axisymmetric conditions and are performed in Plaxis 2D finite element software. The NorSand constitutive model (Jefferies, 1993) is used to characterise the sand behaviour.

2 MODELLING STRATEGY

2.1 Introduction

The numerical analysis presented in this paper is based on Mozaffari et al. (2022). They studied the influence of non-uniformities and end-restrain conditions on the drained triaxial compression response of the Hutchenson Sand, a clean and poorly graded sand with D_{50} of 0.46 mm, C_u of 2.41, e_{min} of 0.55, and e_{max} of 0.88. This work inherits the NorSand parameters calibrated for this material, the pre-shearing state parameters patterns for moist tamping (MT) and perfectly uniform (PU) samples, and the lubricated and rough ends incorporation in the analyses. The main difference is that the undrained triaxial compression behaviour is studied (instead of drained) using a simpler numerical model (e.g. axisymmetric without caps instead of a full 3D with caps).

2.2 NorSand parameters

Table 1 presents the NorSand parameters that Mozaffari et al. (2022) adopted. Given that the Plaxis formulation of the model does not incorporate a void ratio dependency on the reference elastic shear modulus, an average constant value is chosen for this study.

Table 1. NorSand parameters Hutchenson Sand

Symbol	Parameter	Value
$\boldsymbol{G}$ (MPa)	Reference elastic shear modulus	9
$\boldsymbol{\nu}$	Poisson's ratio	0.2
$\boldsymbol{\Gamma}$	CSL void ratio at 1 kPa	0.96
$\boldsymbol{\lambda_e}$	CSL slope in e-ln(p') space	0.038
$\boldsymbol{M_{tc}}$	CSL in p'-q space	1.25
$\boldsymbol{N}$	Volumetric coupling coefficient	0.2
$\boldsymbol{\chi_{tc}}$	Ratio between maximum dilatancy and state parameter	6.0
$\boldsymbol{H_0}$	Initial hardening parameter	310
$\boldsymbol{H_\psi}$	Dependence of hardening on state parameter	2100

2.3 Void ratio non-uniformities

Thompson and Wong (2008) performed CIUC and CIUE tests on Ottawa sand (C778) specimens prepared using moist tamping and water pluviation methods. Using X-ray computed tomography, the authors tracked the initial void ratio patterns and their evolution during shearing. Based on this work, Mozaffari et al. (2022) extrapolated and defined four different non-uniformity void ratio patterns for the Hutchinson Sand: Perfectly Uniform (PU), Moist Tamped (MT), Natural Distribution (ND) and Extremely Non-Uniform (EN). Pre-shearing confining stress of p'=100 kPa was considered along with average state parameters of -0.26 (very dense) and 0.05 (loose) specimens.

This work focuses only on the moist tamping (MT) and perfectly uniform (PU) distributions. Figure 1 illustrates the considered pre-shearing state parameters. PU samples entail uniform values of -0.05, 0.00, 0.05 and 0.10, while MT samples have the same average values but entail variations of $\pm$ 0.04 produced by the layered sample preparation method.

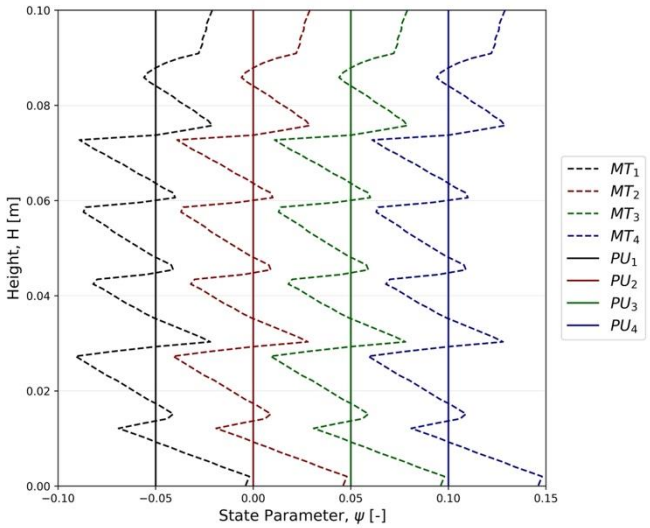

Figure 1. Pre-shearing state parameter distribution for moist tamping (MT) and uniform profile (PU). Adapted from Mozaffari et al (2022).

2.4 Modelling stages

The triaxial tests are modelled using axisymmetric conditions in Plaxis 2D finite element software. A sample radius of 25 mm and height of 100 mm are considered, with 100 horizontal layers subdivisions. Figure 2 illustrates the modelling stages, which are summarised as follows: i) the sample is isotropically consolidated to a mean effective stress of p'=100 kPa using a Linear Elastic (LE) material; ii) a NorSand material is created and assigned to each of the sublayers to represent the correspondent state parameter distribution (as per Figure 1); iii) a prescribed displacement replaces the vertical load and the displacements are reset to zero; iv) undrained shearing is applied by imposing a vertical displacement

of 20 mm (i.e. axial strain of 20%) using a consolidation-type calculation with closed pore pressure boundaries, which allows obtaining a uniform excess pore pressure distribution for the considered shearing rate and permeabilities.

The NorSand materials are activated after the consolidation stage and before the undrained shearing; this is done because NorSand model entail limitations in reproducing compression stress paths. To illustrate, it can generate unexpected plastic deviatoric strains for purely isotropic compression. Therefore, the modelling strategy adopted for this work allows to define the pre-shearing state parameter distributions compatible with those reported in the literature by Thompson and Wong (2008) and Mozaffari et al. (2022), which were adapted for this work (Figure 1).

After running each model, vertical displacements (u_y) and loads (F_y) at the top cap and the pressure (p_b) at the base of the sample are obtained to track magnitudes compatible with laboratory measurements as follows:

$$\sigma_1' = \frac{F_y \cdot 2\pi}{\pi R^2} - p_b \quad (1)$$

$$\sigma_3' = \sigma_c - p_b \quad (2)$$

$$\epsilon_a = \frac{u_y}{H_0} \quad (3)$$

where σ_c is the radial total stress applied at the right boundary, R is the sample radius and H_0 is the initial height.

The lubrication of the end platen is analysed by imposing a free or nil radial displacement at the soil-caps interface, representing the fully lubricated and rough cases, respectively.

Considering the permutation of two lubrication cases, with two sample preparation methods and four pre-shearing average state parameters, a total of sixteen models are performed.

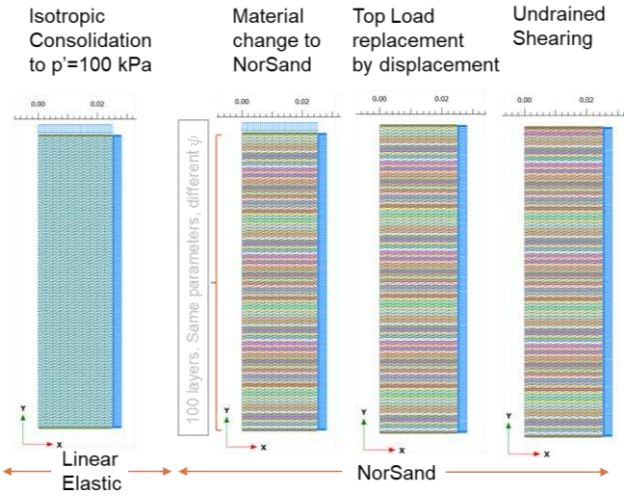

Figure 2. Axisymmetric model in Plaxis 2D. Modelling stages.

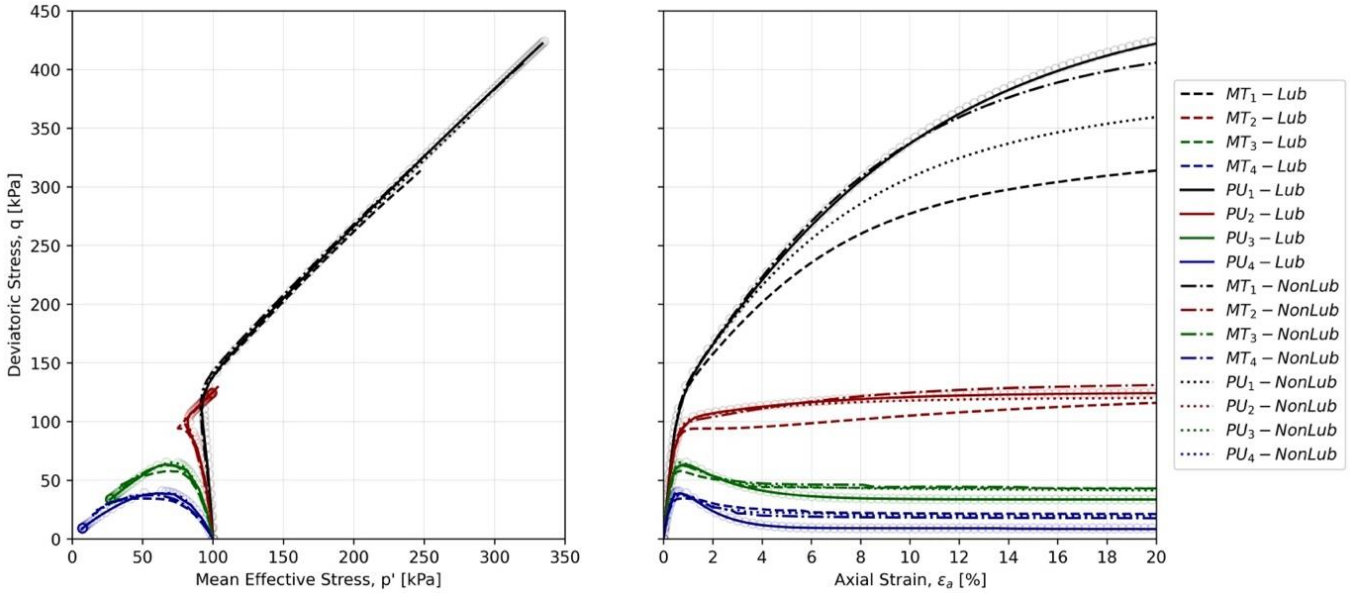

Figure 3. CIUC simulation results, lubricated versus non-lubricated cap. Note: circles represent the elemental test results.

3 RESULTS

3.1 Stress-strain-strength response

Figure 3 displays the effective stress paths ($p' - q$) and the stress-strain ($q - \varepsilon_a$) response for the sixteen analysed cases, interpreted from Equations (1), (2) and (3). Complementary, the results from analogous elemental tests (i.e. single Gauss point) are shown for comparison using coloured circles.

A single Gauss point's stress state is only compatible with a triaxial test if the void ratio is perfectly uniform and the cap is lubricated (i.e. PU-Lub cases). For contractive samples, PU specimens tend to have a more brittle behaviour than MT ones, with lower undrained

residual strengths; particularly, when lubricated caps are used, the sample brittleness is even more pronounced. For dilative samples, PU with lubricated caps entail higher strengths than their MT counterpart; however, this behaviour is inverted when the cap is not lubricated.

3.2 *Undrained shear ratio*

The peak and residual undrained shear strength is obtained for each simulation and subsequently normalised by the pre-shearing effective confining pressure of 100 kPa. Figure 4 and 5 show the peak and residual undrained shear strength ratios (USR) variation with the state parameter of the sample; for clarity purposes, the USR scale is set to a maximum of 1.0 to highlight the behaviour of the looser samples. As expected, the samples entailing positive state parameters achieve undrained residual strengths lower than the peak (i.e. softening occurs); contrary to this, the samples with nil or negative state parameters do not soften (i.e. peak and residual are the same). Moreover, it is observed that the residual shear strength ratios for the ideal case (i.e. PU-Lub) on a loose state (i.e. ψ=0.05 and 0.10) are lower than the values obtained for the other non-ideal cases (i.e. PU-NonLub, MT-NonLub and MT-Lub); a maximum difference of 20% and 50% is observed for ψ=0.05 and 0.10, respectively. This is important, as it can lead overestimation of residual strengths and to different interpretations of the Critical State Line (CSL) for the same material. The differences among the cases are less noticeable when considering the peak shear strength ratio. These results highlight that sample preparation and end platens lubrication plays an important role in the post-peak response of the material.

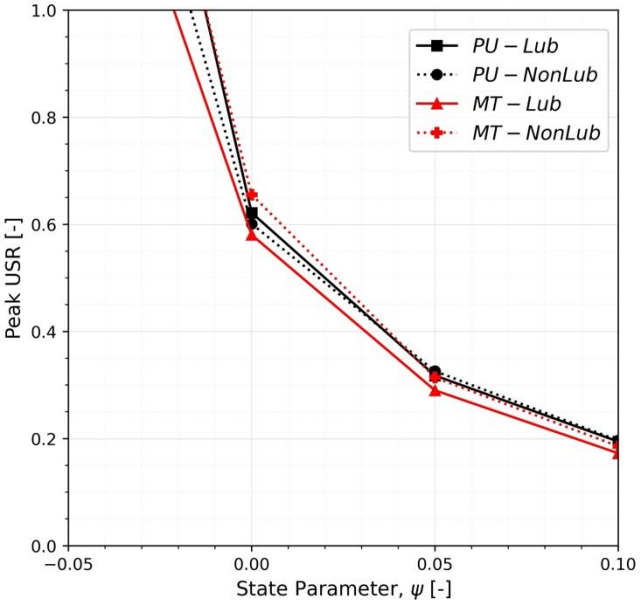

Figure 4. Peak undrained shear strength ratios. Effect of sample preparation and lubrication.

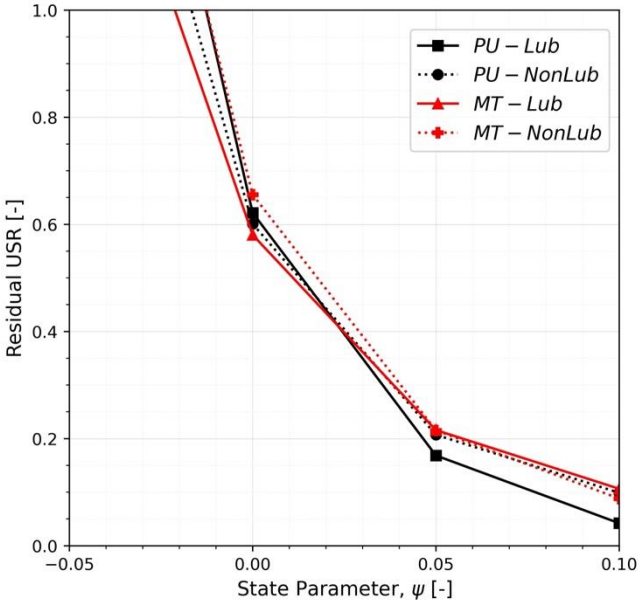

Figure 5. Residual undrained shear strength ratios. Effect of sample preparation and lubrication.

3.3 *Deformed mesh and state parameter distribution at failure for the loosest sample*

Figure 6 displays the deformed mesh at failure for the loosest sample cases (i.e. ψ=0.10). The following observations can be made: i) the PU case with lubrication entails a uniform deformation pattern, as the top edge moves vertically downwards, and the right edge moves radially. No perturbations within the domain are introduced. Thus, strain distribution throughout the sample remains uniform during the simulation, and no strain localisation is encountered. As expected, this case represents a purely academic exercise but is still important to discuss since it is the most typical procedure used to calibrate constitutive model parameters in both industry and academy; ii) the MT case with lubrication entails a local failure at the top region where the state parameter is higher (i.e. looser than average), which might be unrealistic; iii) the PU and MT without lubrication entail local failures at the middle and upper third of the sample height; in both cases, the sample collapses vertically and pushes the material radially, producing the well-known barrel-like failure commonly observed in tests without end lubrication.

Figure 7 shows the state parameter contours at failure for the loosest sample cases (i.e. ψ=0.10). As shown, the ideal case (i.e. PU with lubricated ends) reaches the critical state in the whole specimen as the state parameter approach uniformly to zero. However, all the other cases that entail local failures only reach the critical state in the sheared or localised areas.

The higher volume involved in energy dissipation can explain the lower bound when the sample is loose and the upper bound when the sample is dense, as the specimen can fully contract or dilate, respectively.

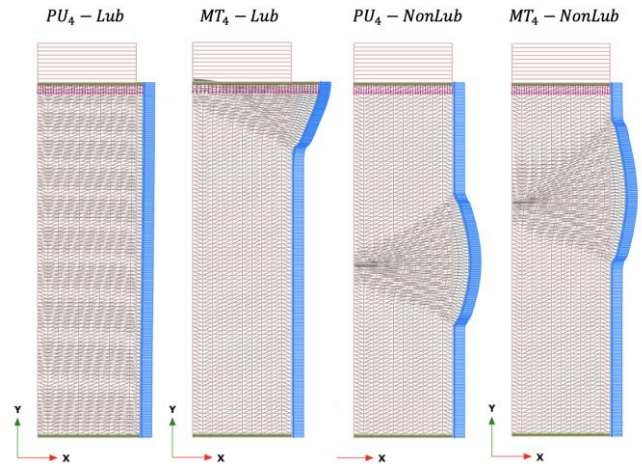

Figure 6. Deformed mesh at the end of shearing, for the loosest specimens (PU_4 and MT_4) for lubricated and non-lubricated cap. Displacements scaled by 0.5x.

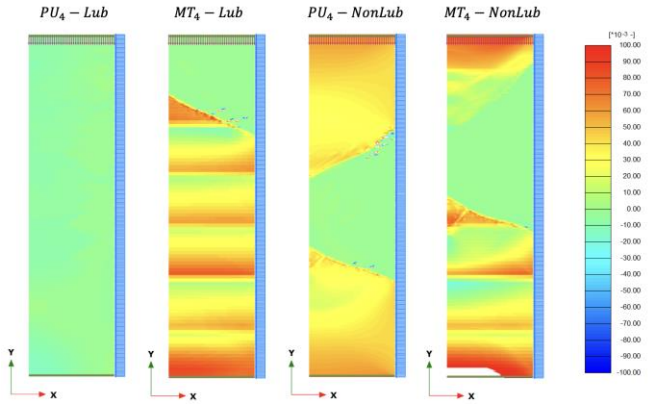

Figure 7. State parameter contours at the end of shearing, for the loosest specimens (PU_4 and MT_4) for lubricated and non-lubricated cap

3.4 Mean effective stress and deviatoric stress distributions at failure for the loosest sample

Figure 8 shows the mean effective stress contours at failure for the loosest sample cases (i.e. ψ=0.10). The ideal case reaches a constant value with minor variations; however, the other cases show noticeable non-uniformities. The non-lubricated samples entail an effective stress reduction above and below the failed areas, driven by a decrease of the minor principal stress due to unloading during failure. Contrary to this, the values are high at the centre and ends.

Figure 9 shows the deviatoric stress contours at failure for the loosest sample cases (i.e. ψ=0.10). Similarly to the mean effective stress, the ideal case reaches a constant value with minor variations, and the other cases show heterogeneities. The decrease of the minor effective principal stress above and below the failed areas leads to increased deviatoric stress in that region. On the other hand, shear bands coincide with the zones with a high gradient on the state parameter depicted in Figure 7. This fact may be useful in the laboratory as the shear band represents the boundary between the portion in the critical state from the other that remained in the initial state.

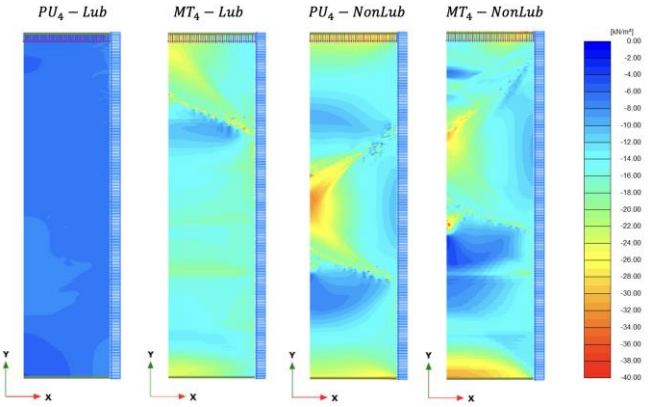

Figure 8. Mean effective stress contours at the end of shearing, for the loosest specimens (PU_4 and MT_4) for lubricated and non-lubricated cap

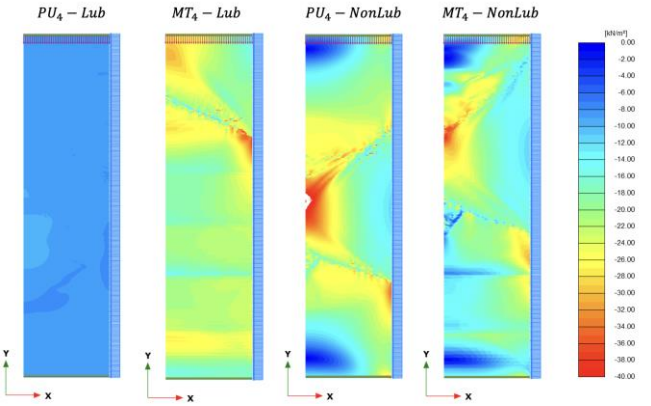

Figure 9. Deviatoric stress contours at the end of shearing, for the loosest specimens (PU_4 and MT_4) for lubricated and non-lubricated cap

4 DISCUSSION AND CONCLUSIONS

The engineering practice of calibrating material parameters typically involves comparing laboratory test results and single material-point simulations, which assumes that stress/strain measurements and the void ratio distribution throughout the sample are uniform. This paper focused on discussing the validity of this assumption.

Numerical simulations were performed to evaluate the impact of the specimen non-uniformities and end restrain conditions on the undrained behaviour of the Hutchenson Sand. A total of sixteen cases were modelled by permutating two lubrication conditions (full and nil), two sample preparation methods (moist tamping and perfectly uniform) and four pre-shearing average state parameters (-0.05, 0.00, 0.05 and 0.10).

Results showed that the stress state of a single Gauss point is only compatible with a triaxial test if the void ratio is perfectly uniform and the cap is lubricated (no shear stress on the boundary), which is practically im-

possible to achieve in the lab. Moreover, when the failures occur locally, it was shown that the residual undrained shear strength ratio can be considerably overestimated, as the volume that dissipates energy is limited, i.e. softening occurs locally, whereas the rest of the sample goes through the unloading branch. On the contrary, the influence on the peak undrained shear strength ratio is less noticeable. These results highlighted that sample preparation and end-platens lubrication plays an important role in the material's post-peak response and, consequently, the set of parameters obtained from the calibration.

Despite being a simple numerical exercise using laboratory data taken from literature, simulations showed that any inhomogeneity embedded in the test (cap friction or sample preparation method) impacts the stress state, modifying the overall mechanical behaviour of the sample and its brittleness. Thus, the results suggested that the state parameter obtained from laboratory tests is not an intrinsic parameter but is strongly dependent on the volume of the sample at critical state ($\psi = 0$) and on the sample stress state.

It must be mentioned that axisymmetric models entail some limitations, as they cannot capture the caps rotations or the localisation along inclined shear bands commonly observed in the laboratory. Moreover, this study does not consider the updated mesh formulation, so the positions of the nodes remain unchanged from the beginning of the testing.

5 REFERENCES

Bishop, A.W. and Green, G.E. 1965. The influence of end restraint on the compression strength of a cohesionless soil. Géotechnique, 15 (3): 243–266.

Elena, P., Lars, I., and Benjaminn, N. 2019. Influence of sample slenderness and boundary conditions in triaxial test - a review. In E3S Web of Conferences. Vol. 92.

Jefferies, M.G. 1993. Nor-Sand: a simple critical state model for sand. Géotechnique, 43(1): 91–103.

Lee, K.L. 1978. End restraint effects on undrained static triaxial strength of sand. Journal of the Geotechnical Engineering Division, 104: 687–704.

Mozaffari, M., Liu, W., and Ghafgazhi, M.2022. Influence of specimen nonuniformity and end restraint conditions on drained triaxial compression test results in sand, Canadian Geotechnical Journal 54, 1414–1426.

Reid, D., Fourie, A.B., Ayala, J.L., Dickinson, S., Ochoa-Cornejo, F., Fanni, R., Garfias, J., Viana da Fonseca, A., Ghafghazi, M., Ovalle, C., Riemer, M., Rismanchian, A., Olivera, R., Suazo, G.. 2021. Results of a critical state line test round robin program. Géotechnique 71: 616–630

Rowe, P.W. and Barden, L. 1964. Important of free ends in triaxial testing. Journal of the Soil Mechanics and Foundations Division 90, 1-27.

Sachan, A. 2011. Shear testing data of soil: a function of boundary friction in triaxial setup. Indian Geotechnical Journal, 41(4): 168–176.

Sheng, D., Westerberg, B., Mattsson, K., Axelsson, K. 1997. Effects of end restraint and strain rate in triaxial tests. Computers and Geotechnics 21(3): 163-182.

Thomson, P.R., and Wong, R.C.K. 2008. Specimen nonuniformities in water pluviated and moist-tamped sands under undrained triaxial compression and extension. Canadian Geotechnical Journal, 45(7): 939–956.

Vaid, Y.P, Eliadorani, A., Sivathayalan, S., Uthayakumar, M. 1999. Discussion of “Quasi-steady state: a real behaviour?” Canadian Geotechnical Journal 36(1): 182-193.